Phase-Locked Antiguided Multiple-Core Ribbon Fiber

Raymond J. Beach, Michael D. Feit, Scott C. Mitchell, Kurt P. Cutter, Stephen A. Payne, Richard W. Mead, Joseph S. Hayden, David Krashkevich, and David A. Alunni

***Abstract*—We report on the first experimental demonstration of a scalable fiber laser approach based on phase-locking multiple gain cores in an antiguided structure. A novel fabrication technology is used with soft glass components to construct the multiple core fiber used in our experiments. The waveguide region is rectangular in shape and comprised of a periodic sequence of gain and no-gain segments having nearly uniform refractive index. The rectangular waveguide is itself embedded in a lower refractive index cladding region. Experimental results confirm that our five-core Nd-doped glass prototype structure runs predominately in two spatial antiguided modes as predicted by our modeling.**

***Index Terms*—Clad pumping, fiber lasers, multicore fiber, phase locking, waveguides.**

I. Introduction

THE DEVELOPMENT of double-clad fiber has brought fiber lasers to the forefront of possible approaches for high beam quality, high average power laser sources [1]. Using a cladding-pumped geometry with a single-mode core, individual fibers have been demonstrated at greater than 100 W of average power [2]. These single-core results are irradiance limited by output facet damage and the onset of deleterious nonlinear optical interactions. Scaling to higher powers requires the area of the laser beam to grow. Two general approaches are actively being investigated for power scaling while preserving single spatial-mode output: 1) large mode area fibers in which the core area is a specially index-engineered waveguide structure [3], and 2) multiple cores which are phase locked to give a single spatial-mode output beam. A number of different techniques have been investigated for phase locking multiple core structures such as evanescent coupling [4], diffractive coupling (Talbot plane methods), and 1-to-N-way phase-locking techniques [5]. With the evanescent technique, the field energy is localized on the gain cores, and nearest neighbor cores are coupled to each other via their evanescent (exponentially decaying) fields. This technique, originally used with multistripe diode lasers [6], has been described in several papers and recently used to phase lock an isometric configuration of seven gain cores in a cladding-pumped fiber [7].

Manuscript received August 28, 2002; revised January 3, 2003. This work was supported by the U.S. AFRL, Albuquerque, under Contract L-8958.1, and by the U.S. Department of Energy under Contract W-7405-ENG-48.

R. J. Beach, M. D. Feit, S. C. Mitchell, K. P. Cutter, and S. A. Payne are with the Lawrence Livermore National Laboratory, Livermore, CA 94551 USA (e-mail: beach2@llnl.gov).

R. W. Mead is with Collimated Holes, Inc., Campbell, CA 95008 USA.

J. S. Hayden, D. Krashkevich, and D. A. Alunni are with Schott Glass Technologies, Inc., Duryea, PA 18642 USA.

Digital Object Identifier 10.1109/LPT.2003.809943

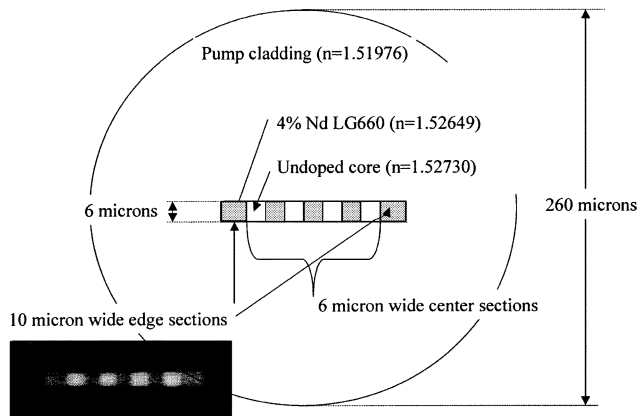

Fig. 1. Cross-sectional diagram of antiguided ribbon fiber structure showing the starting refractive indices of the bulk glass used to construct the fiber preform. Inset photograph shows the waveguide region of the fiber.

II. Experimental Demonstration

The main purpose of this letter is to report on what we believe is the first demonstration of antiguiding to phase lock multiple cores in a fiber structure. Because the eigenmode is delocalized across all gain cores in this scheme, all cores communicate with all other cores and we anticipate scalability will be more favorable than with evanescently coupled structures. Our choice of an antiguided structure is based on an analysis we recently presented on a scalable ribbon fiber concept [8], where we showed that a constant index waveguide region with a periodically modulated gain profile was preferred for ensuring single spatial-mode operation. Single-mode operation is desired so that a static phase corrector alone, placed in the near field of the ribbon laser's output, can optimize the phase across the aperture and result in a high Strehl ratio beam [8]. Fig. 1 depicts a cross-sectional view of the prototype Nd-doped ribbon fiber that we used in our experiments. This structure was fabricated by constructing a fiber preform using bulk LG-660 undoped, and 4% Nd-doped Silicate Schott glasses. The starting refractive index values of the various component glasses were, 1.519 76 for the pump cladding, 1.526 49 for the doped waveguide glass, and 1.527 30 for the undoped waveguide glass. To construct the preform, square and rectangular parallelepiped waveguide component pieces were fabricated and then placed in a cut-out section of the outer cylindrical cladding that was split in a clamshell configuration. The entire preform was then pieced together and held in place by inserting it in a hollow glass containment tube on which a vacuum was pulled during drawing. The preform was first drawn to cane having an outer diameter of 5 mm to facilitate the removal of the outside containment tube, and then the cane

1041-1135/03$17.00 © 2003 IEEE

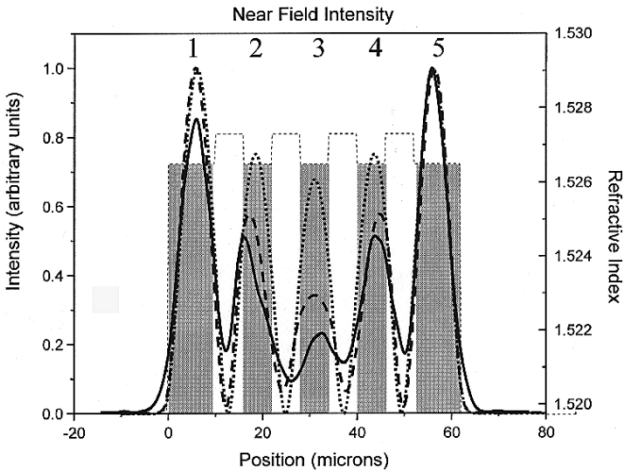

Fig. 2. Near-field measured and model-predicted irradiance profiles. The dotted line is our model-predicted Mode 5. The dashed line is our model-predicted incoherent superposition of Mode 5 and 6 together. The solid line is the experimentally measured near-field lineout. The shaded areas denote those regions doped with Nd^{3+}. The scale on the right references the refractive index profile, shown as a light dotted line.

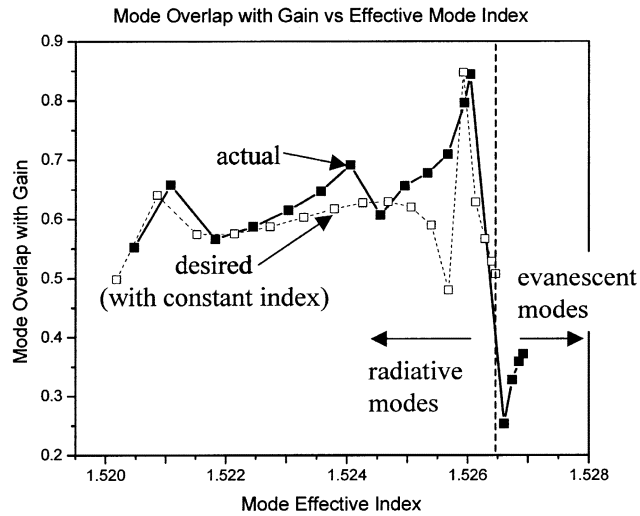

Fig. 3. The dark line is a plot of mode overlap with the gain-loaded portion of the fiber against the effective index value for the various modes supported by the waveguide structure shown in Fig. 1. The dots represent the individual modes. The dashed line is the calculated mode overlap for a waveguide structure similar to the one shown in Fig. 1, but optimized with constant index across the waveguide region.

was drawn to fiber having a final outer diameter of 260 μm. No polymer coating was applied to the fiber.

The spatial-mode structure of the ribbon fiber's output beam was characterized using an end-pumping geometry in which a fiber coupled 808-nm diode array served as the pump source. The output of the diode was imaged into the 260-μm diameter outer cladding of a 1-m-long piece of the fiber having both of its ends polished normal to the fiber axis and uncoated. The pump, which single-passed the fiber, was transmitted through a dichroic mirror contacting the fiber and having high transmission at 808 nm and high reflectivity at 1064 nm. The absorption coefficient of the Nd-doped cores is 5.6/cm at the 808-nm pump wavelength. The 1-m length of fiber was straight and supported by a V-groove machined in a piece of aluminum for the characterizations reported here. Fig. 2 shows a horizontal lineout of the near-field intensity distribution of the fiber superimposed on the index structure of the waveguide. Although this near-field intensity profile was found to be very repeatable, we did observe that arbitrarily bending or otherwise placing stress on the fiber could alter it significantly. Also shown in Fig. 2 are our model-predicted irradiance profiles calculated using the formalism presented in [8] and discussed below. For the index structure shown in Fig. 2, we have also calculated the entire mode spectrum supported by the waveguide as shown in Fig. 3, where mode overlap with the gain region is plotted against mode effective index value. In Fig. 3, radiative modes are defined as those with a harmonic dependence everywhere in the waveguide region, and evanescent modes as those with a harmonic dependence in some areas of the waveguide and an exponential dependence in others, depending on whether the mode index is below or above the local refractive index of the structure, respectively.

To fit our model-predicted modes to the measured near-field irradiance profile we have considered the highest gain mode alone (fifth from the right in Fig. 3), as well as an equal intensity incoherent superposition of the two highest gain modes together (fifth and sixth from the right in Fig. 3). These model-predicted near-field profiles are overlaid with the experimental data in Fig. 2, demonstrating that the two mode superposition replicates the prominent features of the experimental profile better than does the single mode alone. This is not surprising as the fifth and sixth modes are the highest gain modes supported by the structure, but are not well discriminated from each other in their gain overlap values of 0.84 and 0.80, respectively. We believe the remaining disagreement between the experimental results and the model-calculated near-field irradiance profiles can be ascribed to a lack of detailed knowledge of the true refractive index profile of the fiber. The specific refractive index values of the various glass components used in the fiber are known to depend in detail on the cooling rate of the glass during redraw [9], as well as the stress induced in the structure during fabrication, both being uncharacteristic for the glasses used here. While simultaneous operation in two spatial modes is evident here, we note that if a constant index throughout the waveguide region were to be obtained, then the gain discrimination between the most preferred and next most preferred mode would be greatly increased. This is shown in Fig. 3 by the dashed line and open dots, plotting mode overlap against mode effective index for the case of a constant refractive index value of 1.526 49 across the entire waveguide region. In this optimized case, the gain overlap of the two highest gain modes is calculated to be 0.85 and 0.64, substantially better than the mode discrimination in our present fiber.

Fig. 4 shows a horizontal lineout of the experimental far-field irradiance profile of the fiber. The far-field profile was generated by directly focusing the near-field output of the ribbon fiber onto a camera charged-coupled device and digitizing the image, shown as the inset photograph in Fig. 4. Also shown in Fig. 4 is the model-calculated far-field profile generated by propagating the model-calculated near field. Evident in Fig. 4 is agreement between the principal features of the measured and modeled far-field profile indicating there is coherence across the lasing aperture of the ribbon fiber. Contributing to the remaining disagreement between model and experiment is our limited knowl-

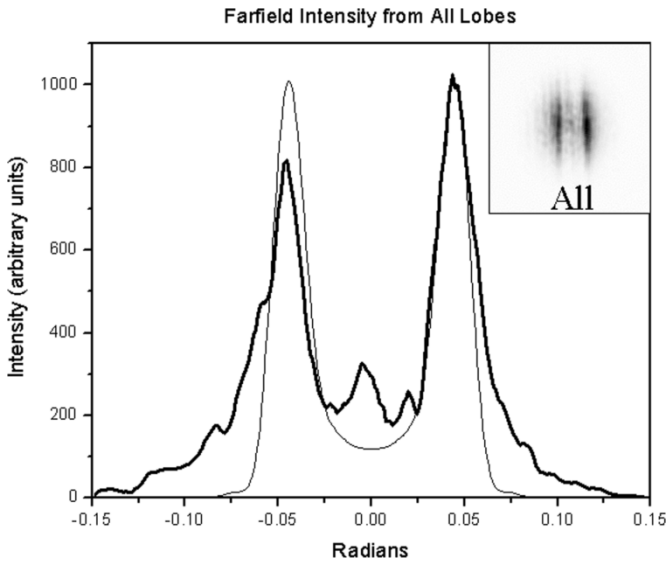

Fig. 4. Darker line corresponds to line out of the experimentally measured far-field irradiance profiles shown in the inset picture, and the lighter line corresponds to the model calculated profile as described in the text.

edge of the detailed refractive index values of the various waveguide components as discussed above, as well as a possible admixture of modes beyond the two used in our modeling due to mode-to-mode scattering [10]. Finally, we characterized the vertical axis (narrow dimension) emission from the ribbon fiber, measuring the M^2 parameter [11] in this dimension to be 2.4, in reasonable agreement with our model prediction of two captured modes in this dimension.

We have also used a 15-cm section of the ribbon fiber as the gain element in a laser oscillator to assess the energetic performance of our antiguided structure, primarily to ascertain the passive loss of the structure under lasing conditions. A 4% reflective output coupling was investigated using the uncoated end of the fiber as the output coupler, and then 10%, 20%, and 30% reflective output couplings were investigated by contacting various flat mirrors to the output end of the fiber. For 4% reflectivity, the measured slope efficiency was 0.24 W/W referenced to the absorbed pump power, and the peak optical–optical efficiency was 0.25 W/W at an absorbed pump power of 3.2 W. System performance using the 10%, 20%, and 30% reflective output couplers was almost constant with a slope efficiency of 0.32 W/W and a peak optical–optical efficiency of 0.25 W/W. Setting the passive loss of the fiber at 0.005/cm, we could reproduce this energetics behavior using a model based on a previously published analysis of end-pumped laser systems [12]. A 1-ms pump pulse was used in these characterizations, and the output radiation from the fiber was observed to be unpolarized with a spectrum extending from 1059 to 1069 nm.

III. Conclusion

We have reported what we believe to be the first demonstration of antiguiding as a mechanism to phase lock a multiple core fiber laser. This demonstration was made using a five-core ribbon fiber structure that was fabricated using a novel soft glass fabrication technology. Although our prototype structure ran predominately in two antiguided modes rather than the desired single spatial mode because of varying refractive index across the waveguide, our experiments have demonstrated that our basic understanding of the optical physics of the device is correct. The benefit of our soft glass approach over a fused silica approach is that it greatly simplifies the fabrication of complicated fiber preforms. However, this advantage has to be weighed against the refractive index control possible with soft glasses. In any case, the soft glass preform has yielded a prototype fiber that has demonstrated the essential novel device physics of a new class of structures. Due to the delocalized nature of their eigenmodes, antiguided structures similar to the ribbon fiber reported here, but with constant index across their waveguide region are being evaluated as potential routes to extremely high power single spatial-mode radiation.

Acknowledgment

The authors would like to thank W. Krupke, J. Dawson, and Z. Liao of LLNL, and L. Brasure and N. Brilliant of the Air Force Research Laboratory (AFRL) for many useful conversations.

References

[1] H. Zeller, U. Willamowski, A. Tunnermann, H. Welling, S. Unger, V. Reichel, H.-R. Muller, J. Kirchof, and P. Albers, "High-power cw neodymium-doped fiber laser operating at 9.2 W with high beam quality," *Opt. Lett.*, vol. 20, p. 578, 1995.

[2] V. Dominic, S. MacCormack, R. Waarts, S. Sanders, S. Bricknese, R. Dohle, E. Wolak, P. S. Yeh, and E. Zucker, "110 W fiber laser," *Electron. Lett.*, vol. 35, no. 14, 1999.

[3] J. Limpert, A. Liem, T. Gabler, H. Zellmer, A. Tunnermann, S. Unger, S. Jetschke, and H. R. Muller, "High-average-power picosecond Yb-doped fiber amplifier," *Opt. Lett.*, vol. 26, pp. 1849–1851, 2001.

[4] N. N. Elkin, A. P. Napartovich, A. G. Sukharev, V. N. Troschieva, and D. V. Vysotsky, "Direct numerical simulation of radiation propagation in a multicore fiber," *Opt. Commun.*, vol. 177, pp. 207–217, 2000.

[5] E. K. Gorton and R. M. Jenkins, "Theory of 1-N-way phase-locked resonators," *Appl. Opt.*, vol. 40, pp. 916–920, 2001.

[6] D. Meyhuys, K. Mitsunaga, L. Eng, W. K. Marshall, and A. Yariv, "Supermode control in diffraction-coupled semiconductor laser arrays," *Appl. Phys. Lett.*, vol. 53, p. 1165, 1988.

[7] P. K. Cheo and G. G. King, "Clad-pumped Yb : Er codoped fiber lasers," *IEEE Photon. Technol. Lett.*, vol. 13, pp. 188–190, Mar. 2001.

[8] R. J. Beach, M. D. Feit, R. H. Page, L. D. Brasure, R. Wilcox, and S. A. Payne, "Scalable antiguided ribbon laser," in *Proc. J. Opt. Soc. Amer. B 19*, 2002, pp. 1521–1534.

[9] H. J. Hoffmann, W. W. Jochs, and N. M. Neurtoth, "Relaxation phenomena of the refractive index caused by thermal treatment of optical glasses below T_g," in *Properties and Characteristics of Optical Glass*. Bellingham, WA: SPIE, 1988, vol. 970.

[10] M. E. Fermann, "Single-mode excitation of multimode fibers with ultrashort pulses," *Opt. Lett.*, vol. 23, pp. 52–54, 1998.

[11] A. E. Siegman and S. W. Townsend, "Output beam propagation and beam quality from a multimode stable-cavity laser," *IEEE J. Quantum Electron.*, vol. 29, pp. 1212–1217, Apr. 1993.

[12] R. J. Beach, "CW theory of quasithree level end-pumped laser oscillators," *Opt. Commun.*, vol. 123, pp. 385–393, 1995.